

## Geophysical key indicators for tailings dam physical integrity monitoring - Brazil

<http://dx.doi.org/10.1590/0370-44672022760030>

**Gilvan Sá**<sup>1,3</sup>

<https://orcid.org/0000-0001-7303-0778>

**Marco Antonio Braga**<sup>2,4</sup>

<https://orcid.org/0000-0002-0244-4655>

**Luiz Antonio Pinto e Almeida**<sup>3,5</sup>

<https://orcid.org/0009-0008-8386-6980>

**Leonardo Santana de Oliveira Dias**<sup>2,6</sup>

<https://orcid.org/0000-0001-5747-8628>

**Alan de Souza Cunha**<sup>2,7</sup>

<https://orcid.org/0000-0001-8458-9235>

**Demetrius Cunha Gonçalves da Rocha**<sup>2,8</sup>

<https://orcid.org/0000-0001-9478-0463>

**Ricardo Luiz Teixeira Telles**<sup>4,9</sup>

<https://orcid.org/0009-0007-2287-8120>

<sup>1</sup>Universidade Federal de Ouro Preto – UFOP, Escola de Minas, Departamento de Engenharia de Minas, Ouro Preto - Minas Gerais - Brasil.

<sup>2</sup>Universidade Federal do Rio de Janeiro - UFRJ, Departamento de Geologia CPGA, Rio de Janeiro – Rio de Janeiro - Brasil.

<sup>3</sup>Centro Federal Tecnológico – CEFET, Araxá - Minas Gerais - Brasil.

<sup>4</sup>Mosaic Fertilizantes, Araxá - Minas Gerais - Brasil.

E-mails: <sup>3</sup>[gilvansa1972@gmail.com](mailto:gilvansa1972@gmail.com),

<sup>4</sup>[marcobraga@geologia.ufrj.br](mailto:marcobraga@geologia.ufrj.br), <sup>5</sup>[almeida0205@gmail.com](mailto:almeida0205@gmail.com),

<sup>6</sup>[leonardo.santana@gmail.com](mailto:leonardo.santana@gmail.com),

<sup>7</sup>[alan.fis@gmail.com](mailto:alan.fis@gmail.com), <sup>8</sup>[demetrius@geologia.ufrj.br](mailto:demetrius@geologia.ufrj.br),

<sup>9</sup>[ricardo.telles@mosaicco.com](mailto:ricardo.telles@mosaicco.com)

### Abstract

The geotechnical monitoring of tailings dams combined with a suitable application of geophysical electrical methods can improve their structure evaluation, allowing several correlations between direct analyses and the resistivity anomaly pattern. Considering this synergy, twenty-three electrical resistivity sections (ERT) were acquired along the beach, abutments, and central part of a dam, totalizing 10,776 m of dataset. After the interpretation of each ERT section, comparing the anomaly ranges with the water level meters measurements, three resistivity zones were defined: Zones of low resistivity (<64 ohm-m), correlated to regions of high humidity; zones of high resistivity (> 357 ohm-m), interpreted as dry zones, and regions with intermediate resistivity values, located between these limits. The groundwater surface generated from the interpretation of the electrical resistivity dataset and the groundwater surface acquired from the water level gauges were almost coincident. On the right abutment, the conductive anomalies showed remarkable continuity, suggesting a high moisture content in this region with strong gradients (200 mV) directed towards the zone of low resistivity values identified in the sections. The analysis showed a robust correlation of the ERT data with localized physical geotechnical measurements, valuable for monitoring dam integrity, overseeing the structure's response to climate and operational changes, and ultimately mitigating the risks of failure. The results of this study support the adoption of a seasonal 4D electrical resistivity survey as an effective tool to monitor and manage surface and high humidity zones, key indicators of dam integrity throughout the entire structure.

**Keywords:** dam monitoring, electrical methods, geotechnical measurements and mining.

## 1. Introduction

A tailings dam is a landfill structure built to store mining waste that consists of liquid, solid or fine particle slurry generated in the ore beneficiation process. Dams are normally built from an initial dike made up of clayey soil and must have potential capacity to store tailings for the life of the mine. According to Chambers (2012), in the past decades, failures of water dams have become extremely infrequent, yet tailings dams have continued to fail with disastrous results. A possible reason is that most tailings storage facilities are typically built and operated incrementally, and partially rely on the tailings themselves for support, unlike water retaining dams, where the dam wall is typically made of concrete or some combination of engineered rock fill and soil and are constructed to their full height before being filled with water and operated.

The application of geophysics in mineral exploration using different methods is a common practice to solve the ambiguity response for most of the mineral deposits worldwide. Geophysics has also been widely applied for the investigation and monitoring of dams in many countries around the world: the USA, Canada, Australia, Japan and some countries in Africa (Dimech *et al.*, 2022). In Brazil, the results of recent research (Malagutti Filho *et al.*, 2018a, 2018b, Da Rocha, Braga & Rodrigues, 2019; Albuquerque *et al.*, 2019; Guirelli Netto *et al.*, 2019) have shown the efficiency of

geophysical methods in the investigation of saturated zones in tailings dams. Zorzi & Rigoti, (2011), published a research article about SP anomalies caused by flow “*per descensum*”, which was used to identify water seepage at concrete dam wall cracks.

The recent increase in the number of accidents involving the rupture of tailings dams has led to search for new methodologies able to improve the risk management of these structures in Brazil. In this sense, geophysical methods can be considered for this purpose as a non-invasive and cost-effective tool with a large application in Engineering/Geotechnical projects (Raji & Adedoyin, 2020).

Inspection and monitoring of tailings dams traditionally include visual inspection and direct measurements using conventional equipment: displacement meters, water level meters (WLM), flow meters, piezometers. Despite the high value information acquired through this workflow, the located nature of these measurements brings some limitations for volume analysis: This dataset is not capable of mapping weakness areas and/or unexpected saturated spots occurring out of the investigation point.

Towards filling this gap in volume analysis, Geophysical Electrical methods applied to tailing dams investigation, such as electrical resistivity (ERT) and self-potential (SP) can complement the traditional methods (Mainali *et al.*, 2015), contributing also to the

geotechnical diagnosis of the dam (Reynolds, 2011). These methods are capable of detecting contrasts of electrical and electromagnetic properties, conditioned by differences in porosity, permeability, presence or absence of interstitial fluids, rock composition and fines concentration (Loke *et al.*, 2013; Boadu & Owusu-Nimo, 2010; Jol, 2008) and are operationally valuable, since they are non-invasive and quickly acquired. Regarding dam volume imaging, ERT methods are capable of inferring humidity anomalies in early and advanced stages, identifying high moisture areas and internal erosive processes (Aal *et al.*, 2004). It is important to emphasize that geophysical methods cannot replace traditional instrumentation. However, this dataset has been extremely valuable to correlate them using 2D and 3D resistivity/humidity models allowing a robust volume evaluation of the dam volume regarding water content. (Martínez *et al.*, 2021; Martínez-Pagán *et al.* 2021).

The main goal of this study is to propose a methodology to map the saturated zones, some moisture content zones and dry zones in the dam structures using electrical resistivity data, applying specific procedures to interpret, zonate and segregate spots by water content. We also investigated the correlation among conductive anomaly shapes in the abutments and central part of the dam and some dynamic changes in the internal hydraulic system of the structure.

## 2. Study area

The study area (Figure 1) is located at Goiás State, midwestern Brazil. The construction of the dam

began in 1982, from a starter dike at 743.0 m above sea level (ASL), subsequently raised in 3 steps. The dam

was raised by the center line method using compacted tailings.



Figure 1 - Overview of tailings dam.

Figure 2 shows the internal drainage system of the dam. Presently, the crest of the dam's maximum elevation is 778.0 m above sea level (ASL). It is 1040 m long and 30 m wide. The

current spillway is located at the left abutment. The downstream slope is protected by superficial vegetation and rainfall water devices. The upstream slope is protected by a tailings beach,

whose width varies between 150 and 200 m.

This type of investigation is named "As is" assessment, detailing the current shape of those structures.

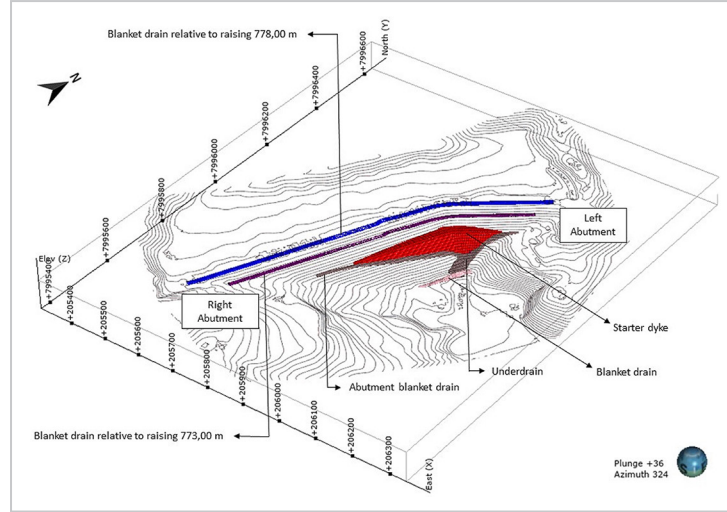


Figure 2 - Structure of the internal drainage and location of the main elements of the dam.

### 3. Physical monitoring instruments and type-sections

Physical monitoring is a set of processes which aims at the observation, detection and characterization of

damages that can offer a potential risk for the dam's safety.

The dam has twenty-six water

level meters (WLM) arranged in its central part and abutments.

### 4. Geophysical data acquisition

#### 4.1 Electrical resistivity – dipole-dipole array

The equipment used in this acquisition was the SupertSting resistivity meter manufactured by AGI using 4-meter electrode spacing, dipole-dipole array and 84 channels with a configuration that reached

depths of approximately 40 to 85 meters. The software employed for data processing and interpretation were: Res2Dinv, Surfer and LeapFrog Geo. The main goal of the electrical geophysical survey was

to segregate saturated zones from the dry ones or with some moisture content, verifying the conductive anomaly continuities, identifying possible seepages, and supervising the internal hydraulic system.

#### 4.2 Data acquisition

For data acquisition, twenty-three survey lines of electrical (ERT) were acquired, adding up to 10,776 m, with electrical resistivity results located along

the beach, abutments, and central part of the dam. All the electrical resistivity sections were acquired in parallel to the dam crest. Twenty profiles of self-potential

(SP) were acquired, adding up to a total 8,472 m of SP data along the dam. The SP profiles were also acquired in parallel to the dam crest (Figure 3).

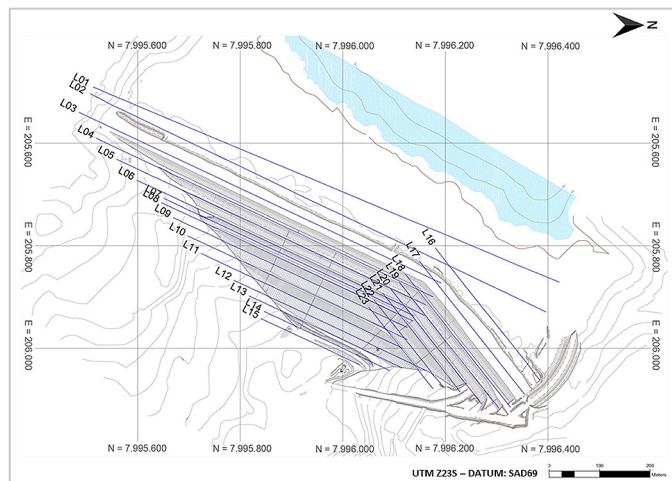


Figure 3 - Location of the 23 ERT sections acquired along the dam.

### 5. Electrical resistivity results

As described in the previous section, a total of 23 ERT sections were acquired along the dam. They were

processed in the RES2DINV software, imported to Leapfrog software, and plotted together with 26 WLM,

distributed along the structure of the dam. Figure 4 presents an example of this analysis:

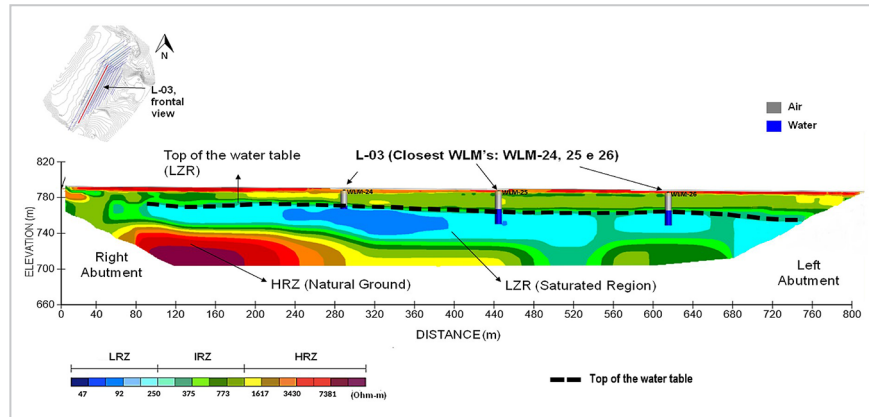


Figure 4 – Example of a non-constrained ERT section (2D view)

with all WLMs projected over the plane of the section. Aiming to establish a robust correlation, we discarded all WLM located far from the section and kept just the ones indicated by the arrows to perform the color range analysis.

Figure 4 presents the strong correlation from the top boundary of the low resistivity zones (LRZ) and water level from WLM. The water table extracted from the data collected by the WLMs was compared to the surface interpreted from the non-constrained electrical resistivity dataset in all the other sections and the correlations defined a new ERT color range, represented

by a new color table (Figure 5), focusing to extrapolate the “Geophysical WLM” to the whole structure, specially where WLM are not installed. Aiming to keep the accuracy of the comparison, we chose just WLMs measurements taken in the closest period to Electrical data acquisition.

From these analysis, the electrical resistivity sections reached depths of ap-

proximately 40 to 85 meters. In general, it was possible to separate the resulting zones of low resistivity (LRZ) (< 64 ohm-m), identified as being saturated or high in moisture content. High resistivity zones (HRZ) (> 357 ohm-m), identified as dry regions, and regions with some moisture content, classified as intermediate zones (IRZ), located between these limits (Figure 5).

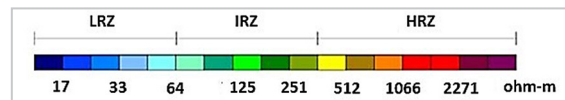


Figure 5 - Scale of electrical resistivity values of dam.

The complete dam electrical imaging was obtained from the 3D plot of the 23 ERT sections using the new

color table (Figure 6). Through the 3D imaging, it was possible to separate the dry regions from the saturated

zones by studying the hydraulic behavior of the dam.

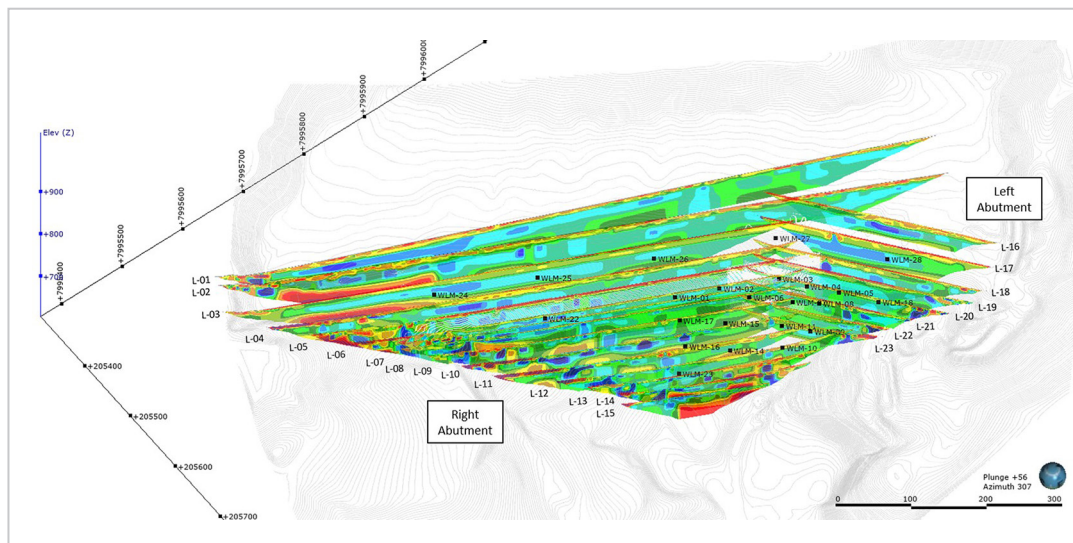


Figure 6 - 3D view with the 23 ERT sections obtained along the dam. This figure also shows the position of the WLM.

When applying the new color table in L-03 and all the other ERT sections, the correlations between LRZ and dam water level were remarkable (Figure 7).

The top of the low resistivity zone (LRZ) ( $< 64 \text{ ohm-m}$ ) was interpreted as being the top of the water table. In L-03, it is now possible to observe the remark-

able coincidence the 24, 25 and 26 water level meters (WLMs), closer to the section, and the position of the water table surface inferred from the electrical resistivity data.

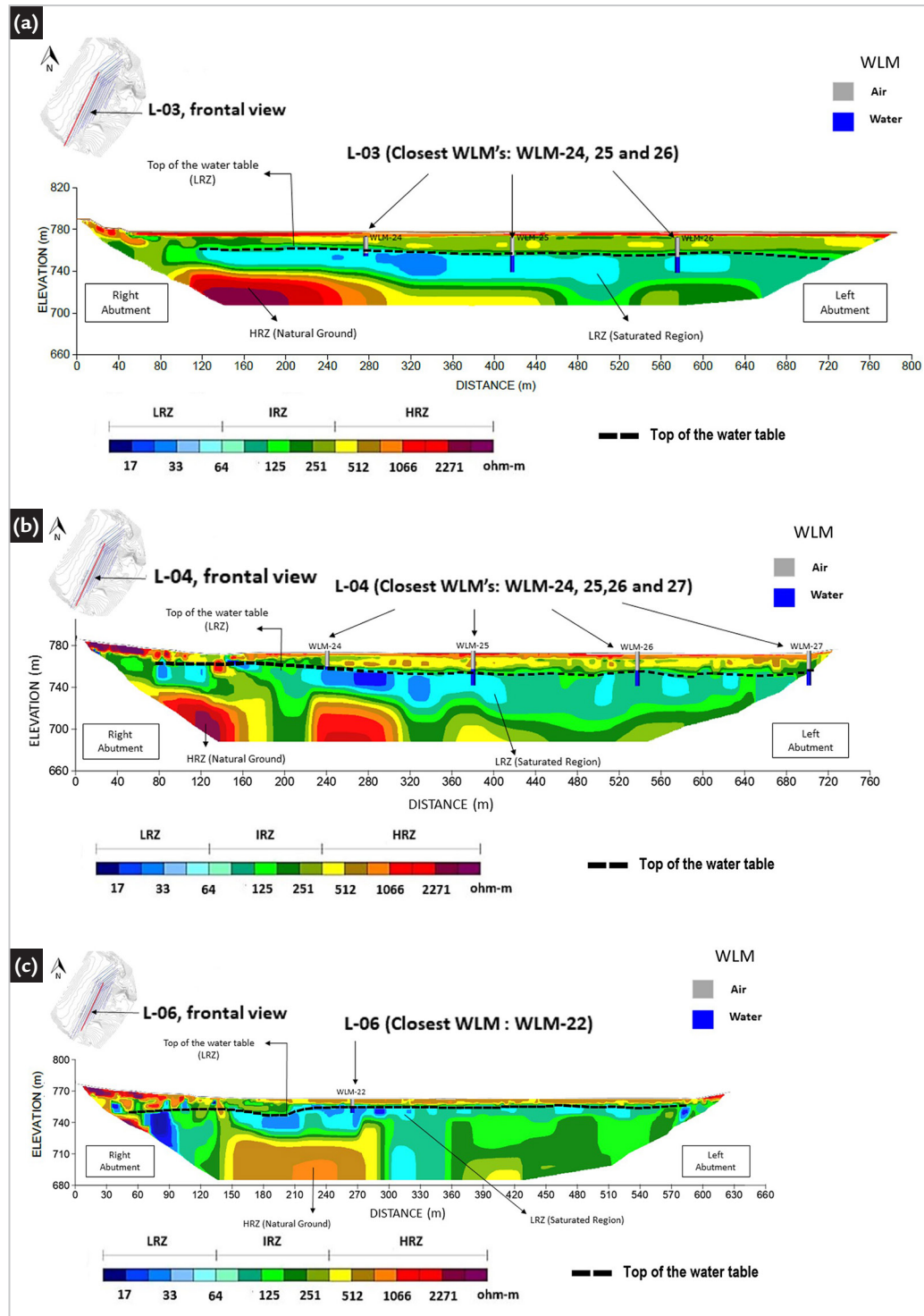


Figure 7 - Sections L-03, L04 & L06 showing the water table outline from the electrical resistivity data (LRZ) and comparing with WLM measurements.

For comparison purposes, the water table position, interpreted from the electrical resistivity results was plotted in relation to the one inferred from the WLMs. It was possible to

observe proximity of the results from the direct and indirect measurements provided by the geophysical surveys RMS. Therefore, with the 3D dam view, it was possible to outline all

the tops of the low resistivity zones (LRZ) from the 23 acquired sections of electrical resistivity (ERT) and to infer a continuous water table surface inside the dam (Figure 8).

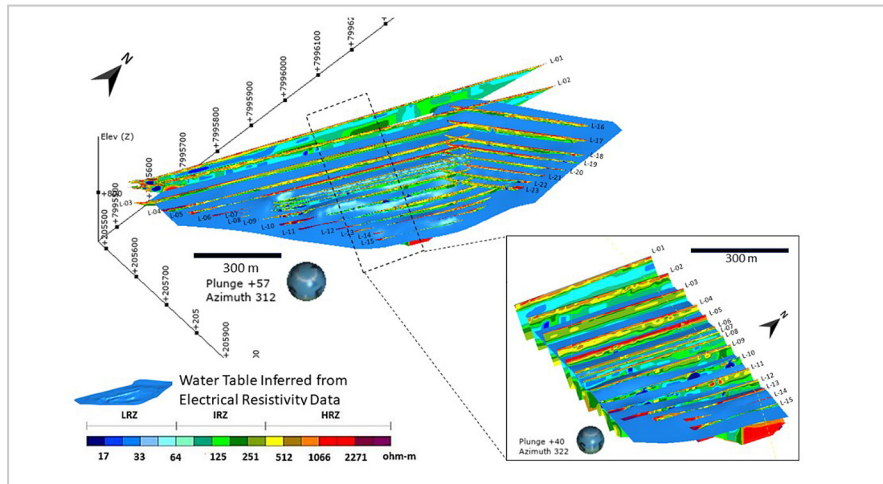


Figure 8 - Water table surface modeled from de ERT data. 3D view of the water table surface along with the geophysical electrical resistivity sections.

### 5.1 Right abutment investigation

Following the analysis using the proposed workflow, some low resistivity zones (LRZ) were mapped in the right abutment of the dam. These anomalies were mainly located in the contact between the earth-fill and the natural

terrain (HRZ). These anomalies, almost vertical, display a remarkable continuity throughout the sections L-04-07-09-11-15, and suggest the presence of subsurface water (Figure 9). In figure 10, another analogous behavior was mapped in

sections L-10-11-12-13, where a high electrical conductivity zone (LRZ), marked with a dashed line, also suggests the presence of subsurface water, below the secondary drainage along this region.

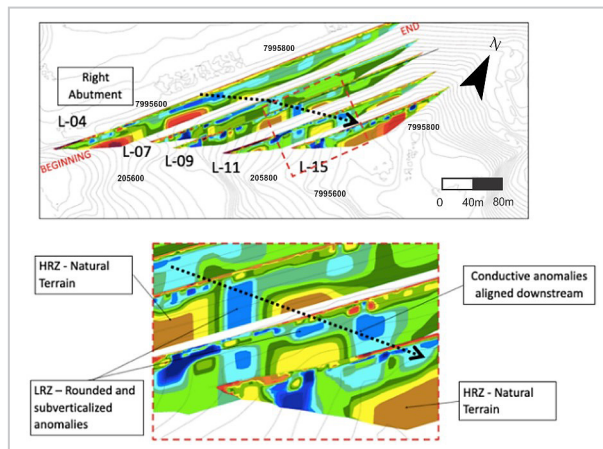


Figure 9 - Highlighting the sections L-04, L-07, L-09, L-11, L-15, closest to the right abutment. The figure shows the conductive anomalies alignment suggesting the presence of water in this region.

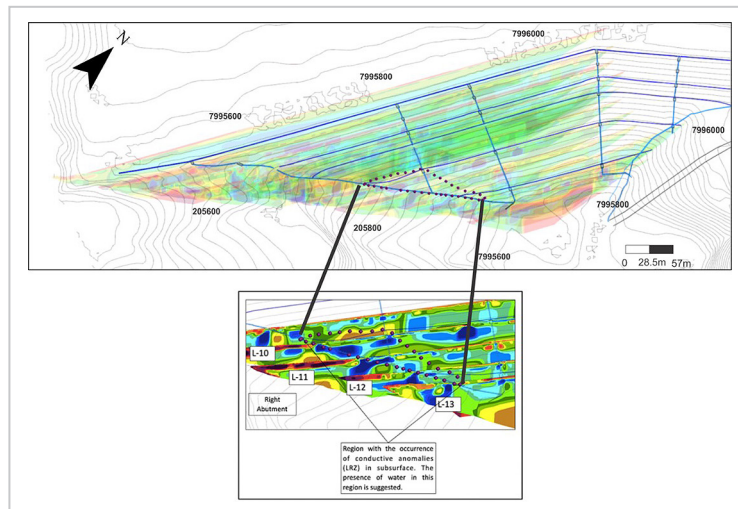


Figure 10 - Sections L-10, L-11, L-12 and L-13 in detail, showing the right abutment and the conductive anomalies in the subsurface. The blue lines represent the dam's drains.

It is important to highlight the position of the blanket drain in the abutment. It is displayed together with the L-07 electrical resistivity section in

Figure 11, and it can be observed that this draining structure has a highly conductive region over an intermediate resistivity zone (IRZ). These high electrical

conductivity zones (LRZ) will assist on the installation of new monitoring instruments and serve as input for geotechnical projects.

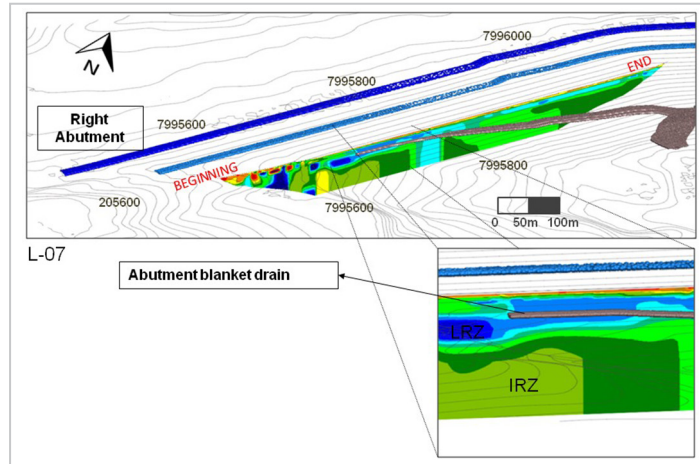


Figure 11 - The abutment blanket drain within a high conductivity region (LRZ). At the right end, an increase on LRZ is observed. There is a possible presence of water in this region.

### 5.2 Electrical modeling and investigation points

The modeling of the ERT data allowed to determine the position of geotechnical features of interest, or investigation points, presenting the associated volumes and their georeferenced

coordinates (Figure 12). After this step, an implicit result model was generated through the coordinates of each conductivity zone marked on each ERT profile. Next to the right abutment, a region of

high electrical conductivity (LRZ) was mapped, evidenced by the geophysical sections. Near the dam crest, at the left abutment, local volumes were also marked to be further investigated.

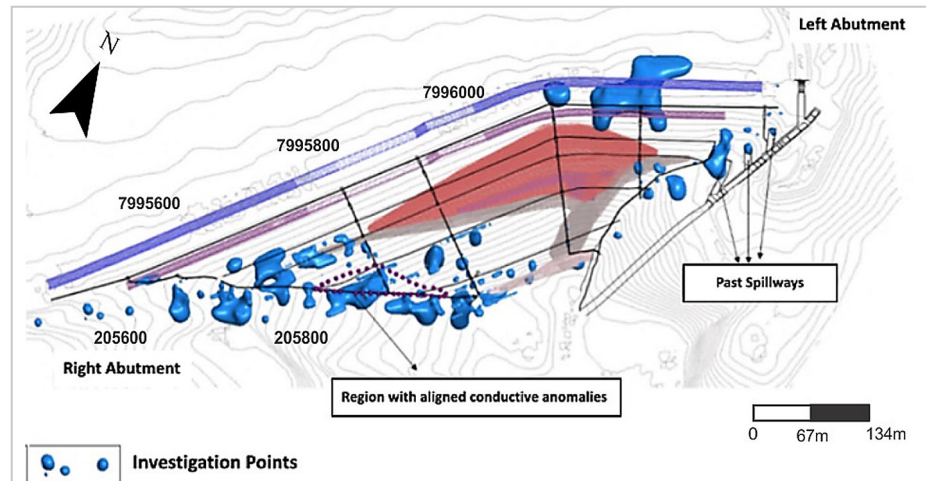


Figure 12 - ERT dataset modeling and investigation zones, key indicators for high moisture zones.

## 6. Conclusions

From the geophysical surveys, we generated continuous 2D and 3D views of the conductivity anomalies mapped in the dam volume, producing a complete imaging along the central part and abutments. ERT results showed a good ability to infer the water table surface, internal hydraulic dynamics, local saturations, and were useful for identifying the main discontinuities among the materials used during the dam wall heightening stages. In general, the electrical resistivity method proved to be the one that best differentiates dry zones (HRZ) from saturated zones

(LRZ) or zones with some moisture content (IRZ). The interpretation phase emphasized the continuity between conductive anomalies in the abutments and central part of the dam identification being made possible by systematically mapping of the entire internal hydraulic system.

This study confirmed that geophysical investigation is also a valuable tool to confirm internal dam structures: internal drains, starter dyke and, in special cases, the boundaries of the dam composing materials.

The next steps will be to define the

key safety indicators based on geophysical dataset and the results of field investigation. Repeatability will be keen to monitor the evolution of the saturated zones in response to the dam operation and whether there are any changes. Other geophysical methods, like MASW (Multichannel Analysis of Surface Waves) and microseismic sensors can be also important to solve some interpretation ambiguity and diversifying physical properties for mapping the dam structures under the same environmental conditions.

## Acknowledgments

We would like to thank Centro de Pesquisa em Geofísica Aplicada (CPGA) from Universidade Federal do Rio de Janeiro - UFRJ, for all support in this research.

## References

- AAL G. Z. A.; AHMED, M. I.; ANDERSON, N. L.; ATEKWANA, E. A. Geophysical investigation of seepage from an earth fill dam, Washington County, MO. *Journal of Applied Geophysics*, v. 44, p. 167-180, 2004.
- ALBUQUERQUE, R.; BRAGA, M. A.; OLIVEIRA, L. A.; DIAS, L. S. O.; ALMEIDA, L. A. P.; OLIVEIRA, A. H.; BRANDÃO, S. Caracterização de barragens de rejeito usando geofísica rasa: aplicação na Barragem B1 de Cajati, São Paulo. *Anuário do Instituto de Geociências*, v. 42, p. 567-579, 2019.
- BOADU, F. K.; OWUSU-NIMO, F. Influence of petrophysical and geotechnical engineering properties on the electrical response of unconsolidated earth materials. *Geophysics*, v. 75, n. 3, p. g2-g29, 2010.
- CHAMBERS, D. Long term risk of releasing potentially acid producing waste due to tailings dam failure. *In: INTERNATIONAL CONFERENCE ON ACID ROCK DRAINAGE - ICARD*, 9, 2012, *Proceedings [...]* Ottawa ON, Canada, v. I, p. 528-539.
- DA ROCHA, D. C. G.; DA SILVA BRAGA, M. A.; RODRIGUES, C. T. Geophysical methods for BR tailings dam research and monitoring in the mineral complex of Tapira-Minas Gerais, Brazil. *Brazilian Journal of Geophysics*, v. 37, n. 3, p. 275-289, 2019.
- DIMECH, A.; CHENG, L.; CHOUTEAU, M.; CHAMBERS, J.; UHLEMANN, S.; WILKINSON, P.; MELDRUM, P.; MARY, B.; FABIEN-OUELLET, G.; ISABELLE, A. A review on applications of time-lapse electrical resistivity tomography over the last 30 years: perspectives for mining waste monitoring. *Surveys in Geophysics*, v. 43, n. 6, p. 1699-1759, 2022.
- GUIRELI NETTO, L.; GANDOLFO, O. C. B.; MALAGUTTI FILHO, W. ; MOREIRA, C. A.; DOURADO, J. C.; CAMARERO, P. L. . 3D geophysical investigation from the methods of electro resistivity, self-potential and seismic refraction in an earth dam. *In: NEAR SURFACE GEOSCIENCE CONFERENCE & EXHIBITION*, 2019, The Hague, Netherlands. EUROPEAN MEETING OF ENVIRONMENTAL AND ENGINEERING GEOPHYSICS, 25, 2019. *Proceedings [...]*.
- JOL H.M. (ed.). *Ground penetrating radar theory and applications*. Burlington, MA: Elsevier, 2008. 545 p.
- LOKE, M. H.; CHAMBERS, J. E.; RUCKER, D. F.; KURAS, O.; WILKINSON, P. B. Recent developments in the direct-current geoelectrical imaging method. *Journal of Applied Geophysics*, 95, 135-156, 2013.
- MAINALI, G.; NORDLUND, E.; KNUTSSON, S.; THUNEHED, H. Tailings dams monitoring in Swedish mines using self-potential and electrical resistivity methods. *Electronic Journal of Geotechnical Engineering*, v. 20, n. 13, p. 5859-5875, 2015.
- MALAGUTTI FILHO, W.; DOURADO, J. C.; MOREIRA, C. A.; COURA, M. M.; BERGONZONI, F. A. Study of small earthfill dams structure using seismic refraction, ERT and self-potential methods. *In: EUROPEAN MEETING OF ENVIRONMENTAL AND ENGINEERING GEOPHYSICS NEAR SURFACE GEOSCIENCE*, 24, 2018a. Porto, Portugal. *Proceedings [...]*.
- MALAGUTTI FILHO, W.; MOREIRA, C. A.; DOURADO, J. C.; COURA, M. M.; GUIRELI NETO, L. Emprego integrado de métodos sísmicos e geoeletricos no estudo de barragens de terra de pequeno porte. *In: SIMPÓSIO BRASILEIRO DE GEOFÍSICA*, 8, 2018, Salinópolis, PA: SBGf, 2018b. *Proceedings [...]*.
- MARTÍNEZ, J.; MENDOZA, R.; REY, J.; SANDOVAL, S.; HIDALGO, M. C. Characterization of Tailings Dams by Electrical Geophysical Methods (ERT, IP): Federico Mine (La Carolina, Southeastern Spain). *Minerals*, 11, 145, 2021. <https://doi.org/10.3390/min11020145>.
- MARTÍNEZ-PAGÁN, P.; GÓMEZ-ORTIZ, D.; MARTÍN-CRESPO, T. *et al.* Electrical resistivity imaging applied to Tailings Ponds: an overview. *Mine Water and the Environment*, 40, 285-297, 2021. <https://doi.org/10.1007/s10230-020-00741-3>.
- RAJI, W. O.; ADEDOYIN, A. D. Dam safety assessment using 2D electrical resistivity geophysical survey and geological mapping. *Journal of King Saud University - Science*, v. 32, n. 1, p. 1123-1129, 2020. <https://doi.org/10.1016/j.jksus.2019.10.016>.
- REYNOLDS, J. M. *An introduction to applied and environmental geophysics*. 2. ed. Chichester: John Wiley & Sons, 2011. 712 p.
- ZORZI, R. R.; RIGOTI A. Aplicação de métodos geoeletricos para monitoramento da barragem de concreto da UHE Gov. José Richa. *Boletim Paranaense de Geociências*, v. 65, 2011.

---

Received: 10 May 2022 - Accepted: 27 June 2023.